Journal of Advanced Zoology
ISSN: 0253-7214
Volume 44 Issue S7 Year 2023 Page 1454:1462

Pre Processing Of Paddy Leaf Disease Using Laplacian Filter

U. Lathamaheswari[1]*, J. Jebathagam[2]

[1]*Department of computer science Vels Institute of Science Technology and Advanced Studies Chennai, India. Email: lathasukumar1812@gmail.com
[2]Department of computer science Vels Institute of Science Technology and Advanced Studies Chennai, India. Email: jthangam.scs@velsunive.ac.in

***Corresponding author:** U. Lathamaheswari
*Department of computer science Vels Institute of Science Technology and Advanced Studies Chennai, India. Email: lathasukumar1812@gmail.com

Article History

Received:
Revised:
Accepted

Abstract

Automatic leaf disease detection in precision agriculture using the images of infected leaves using image processing, computer vision, and machine learning algorithms to determine the presence of illness. The automatic disease detection makes the farmer with accurate plant disease diagnosis that allows the completion of diagnosis procedure. It took a long time for the farmer to send in a stained leaf, where a pathologist confirmed the disease. Upon delayed response, there exist a reduction in the productivity of crop. Automating the disease detection is essential for diagnosis of agricultural diseases. In this paper, we improve the pre-processing operations of the images using Laplacian filter that removes the unwanted noises. The simulation is used to evaluate the proposed pre-processing and feature extraction with existing state-of-art methods. The simulation results suggest that the proposed method is more effective than other ways in enhancing the level of accuracy in diagnosing the entire plant.

Keywords—Precision agriculture, Disease detection, Classification, Machine learning.

I. INTRODUCTION

Farming has an important role in providing food for the world population, which includes both humans and cattle. For example, the usage of biodiesel fuels has expanded agriculture function to include the generation of renewable energy sources such as wind and solar. Textiles, chemicals, and pharmaceuticals are all dependent on agricultural inputs for their production. Despite the fact that agricultural land use increased by only 10% between the 1960s and the turn of the century, agricultural output tripled [1]. Farm mechanization, higher productive crop and livestock breeds, as well as the usage of pesticides and fertilizers, have all been suggested as explanations for the rise in production. The increase in agricultural productivity has slowed significantly in recent years [2].

A gain in agricultural output will be the most effective strategy for easing food insecurity in the future, given that agricultural land will only account for a small proportion of the planet landmass in the future [3]. It will be necessary to develop crop and livestock varieties that are faster maturing, higher yielding, disease resistant

and drought in order to achieve this goal. When it is predicted that the global workforce will reduce by 30% as a result of higher-paying jobs in other industries [4], agriculture must embrace technology now more than ever. It should be clear to anyone who is interested after reading this that the success of the disease recognition algorithm will be determined by a variety of variables over which the algorithm designer will have final say. Approaches to image preprocessing and segmentation, color spaces, feature extraction, and learning algorithms are only a few of the topics to take into consideration. The ideal combination of preprocessing, feature extraction, and classification algorithms cannot be predicted a priori when using feature extraction to automatically detect plant pathogens in a given dataset.

On top of that, customized solutions fall short when operational conditions alter even a little bit from their initial configurations. According to a study, segmentation algorithms can yield misleading findings when dealing with intricate backdrops and lesions that do not have well-defined borders or borders that are poorly defined. Furthermore, some of the most useful characteristics for categorization cannot be recovered manually using any of the currently available mathematical procedures.
According to a recent study, there has been an upsurge in studies that use both pre-and post-processing approaches, where pre-processing best prepares input for a deep learning network and post-processing best optimizes output.

Preprocessing procedures are sometimes used to identify and manage artefacts in histopathology images, while post-processing methods are used to minimize network prediction errors even further in some cases. There are two possible causes of error in network prediction: spontaneous occurrences and the inherent restrictions of the neural network model. When doing classification tasks, for example, it is possible to make use of the spatial interactions between nearby patches or sub-images to change the prediction of the network.

However, because of the irregularity of manual sectioning and the fading of stains with time, the existing method does not provide perfect consistency. The color appearance of samples varies between laboratories. These inconsistencies between the appearance of the tissue and the appearance of the stain make quantitative tissue analysis more challenging.

Given the current restrictions of digital pathology, specific preprocessing and data curation procedures are required in order to train a stable deep learning model. Many preprocessing approaches have been developed in recent years with the goal of eliminating the artefacts associated with standard methods of histology slide preparation. Whenever we talk about preprocessing, the studies are referring to all of the techniques that are used to increase the quality of the network input before it is passed to the final model.
In this paper, we use how a Laplacian filter can be used to remove unwanted noise from image preprocessing. A computer simulation is used to evaluate the proposed methodologies for preprocessing and feature extraction, and the results are presented. According to simulation data, this technique looks to be superior to others in terms of boosting the accuracy of diagnosing the entire plant, as opposed to other strategies.

II. RELATED WORKS

Calderon, S., et al. [11] investigated the use of digitised X-ray images of the hands to estimate the age of a person using a convolutional neural network. Using the Deceived Non Local Means (DNLM) filter, they studied the impacts of denoising, contrast, and edge enhancement on a variety of images. The two parameters of the DNLM filter can be used to regulate the edge enhancement and denoising effects. The accuracy of the CNN-based model regression was tested at various contrast augmentation and denoising settings, and the results were promising. It was discovered that contrast enhancement was useful for preprocessing in a CNN-based technique by using a larger publicly available dataset, resulting in a statistically significant 42% lower root mean squared error and findings that were equivalent to the previous state of the art.

An approach presented by Choi, H., and Jeong, J. [12] that uses speckle reduction anisotropy guided filter and soft thresholding to remove noise from images by preserving the edge information. This filter is applied to a noise image in order to obtain a filtered image, which is then processed further. A logarithmic adjustment is made to the filtered image in order to further reduce the amount of multiplicative noise that is still there. In order to break down the filtered image into several resolutions, the discrete wavelet transform (DWT) was applied. Our method of selecting subimages with high and low frequencies was guided filtering, followed by

soft thresholding. A DWT is applied to the denoised image, followed by an exponential transform and an inverse DWT, as needed.

Khan, K. B., et al. [13] proposed a new parallel approach for denoising and extracting blood vessels from retinal images, which they call the Parallel Approach. The multiscale Frangi filtering technique is used to improve the appearance of vessels with different diameters. Raster to vector transformation is employed in post-processing in order to generate an accurate vessel location map (VLM). A novel post-processing technique is applied to remove misclassified vessel pixels from the image. To produce the final segmented image, an AND operation between the VLM and Frangi output images is performed pixel-by-pixel on both images.

A low-arithmetic smoothing model, as well as a power-efficient strategy for anisotropic diffusion smoothing, were developed following the publication of Nair, R. R., et al. [14]. Based on standard performance, it is clear that this approach performs far better than the basic robust smoothing approaches.
S. Shabeer et al. [15] proposed doing preprocessing on magnetic resonance imaging (MRI) images to detect disease. The advent of segmentation and classification algorithms in the field of magnetic resonance imaging (MRI) has made tumour detection much easier. On the other hand, the segmentation time, PSNR and accuracy of existing techniques, on the other hand, have stayed unaltered.

Yang, W., et al. [16] uses a modified Kalman filter-based scalloping suppression technique that was preprocessed before use. Scalloping is first investigated through the creation of an image model. With the help of a modified Kalman filter, it is possible to assess the strength of scalloping. However, when dealing with complicated scenarios or when the scalloping effect is significant, the Kalman filter performs badly. It is therefore necessary to introduce a novel image preprocessing technology, which combines segmentation with pixel value filling, to the market. Finally, satellite images of a variety of scenes are used to verify the technique that has been proposed.

It was discovered that an ensemble preprocessing strategy provided by Bnouni, N., et al. [17] might increase the performance of a CNN for cervical cancer segmentation. This paper discusses methods for histogram-based image processing, smoothing, and morphological image processing. Following that, we constructed three CNNs based on the same concept. Each of the three preprocessed datasets is used to train a distinct convolutional neural network. We used a left-out testing image sample to construct a probability segmentation map for each CNN, which was then cross-validated using the remaining images in the training set.

III. METHODOLOGIES

As shown in Figure 1, a Laplacian filter is employed to preprocess the grayscale image first, followed by the application of adaptive histogram equalization (AHE) on the preprocessed image, as shown in Figure 1. An edge-sharpening filter is a type of filter that improves the sharpness of the image edges.

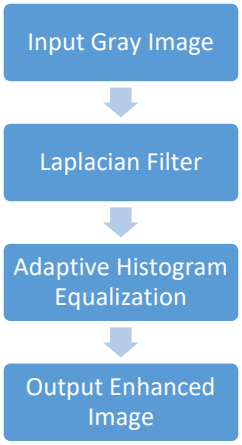

Fig. 1. Proposed process of Image Pre-Processing

In order to limit the amount of memory and computational resources required, the images in the dataset are scaled and cropped to a size of 300x450 pixels during preprocessing. The removal of the image background, which is accomplished through the use of hue values-based fusion, is a vital stage in this process. The image

is first converted from RGB to HSV color space. Because it is greater than whiteness, the S value in the HSV model is taken into consideration first. For the purpose of creating a mask, the RGB image is merged with the binary image formed using the threshold value of 90. The threshold value is tested in a number of different ways before a final decision is made on the value. The backdrop is removed from the image during the fusion process by setting the pixel values to 0. In the RGB color space, a pixel with a value of 0 represents the absence of color. Only the diseased region of the leaf can be seen in this shot, which has been cropped to remove the backdrop. In Fig. 3, the preprocessing procedures are depicted.

A. Laplacian filter for Noise Removal

In image enhancement, the Laplacian function is a second-order derivative method to enhance the image. It identifies the smallest of details in an image. When applied to a feature that has an abrupt discontinuity, the Laplacian operator will enhance it. It is well known that the Laplacian operator is a linear differential operator that approximates the equation as in eq. (1)

$$\nabla^2 f = \frac{\partial^2 f}{\partial x^2} + \frac{\partial^2 f}{\partial y^2} \qquad (1)$$

where f – input image

B. Adaptive histogram equalization (AHE)

The usual strategy for histogram equalisation is to remap the image grey scales in such a way that the resulting histogram resembles a histogram with a uniform distribution. A unique gray-scale mapping is used to provide the same improvement for all portions of an image, even if the photos have different image quality. When performing its transformation, the GHE makes use of the histogram data from the entire input image. First, the histogram of the image is produced, and then the cumulative distribution function (CDF) is generated for the image. As a result of its inability to retain the local brightness image properties, this enhancement technique is not suitable for enhancing the entire photograph. When compared to the original image, GHE results in mild contrast stretching in some dominant grey levels with larger image components and significant contrast loss in other smaller ones in the grey image, which is composed of both higher- and lower-frequency components. Due to the fact that grayscales differ from one place to another, this concept is no longer valid.

As previously stated, an adaptive histogram equalisation (AHE) technique must be utilised since the contrast enhancement mapping of an individual pixel is controlled by the intensity values surrounding the pixel. This step, which is an extension of the conventional histogram equalisation technique, must be done for each pixel in the image in order to be effective. The contrast of each tile is enhanced, and the nearby tiles are blended together using bilinear interpolation to eliminate false boundaries in order to get a more seamless appearance. It divides the image into multiple regions and applies the histogram equalisation operation to each of them. For GHE to be effective, this technique must be applied to each and every pixel in the image, which is not possible with other techniques.

There are two types of histogram equalisation algorithms: nonadaptive and adaptive. Nonadaptive equalisation procedures are the most common. In a nonadaptive algorithm, each pixel is altered by applying the same pattern of calculation that was used to create the histogram of the entire image in a nonadaptive method. When using nonadaptive histogram equalisation procedures, high-quality images are prone to degradation. Adaptive algorithms change the appearance of each pixel based on the pixels in the vicinity of the pixel location in space. The contextual area is a term used to describe this section of the body. The computation of adaptive histogram equalisation necessitates a significant amount of computational power. Certain new procedures were developed in order to make the original process even more efficient.

An image with n×n resolution, with k intensity levels, and a contextual area of m×m is processed in O (n+k) twice the amount of time as an image with O(n^2(m+k)) resolution and k intensity levels. Interpolating the mappings of the four nearest points is used to change each pixel by interpolating the mappings of the four nearest points.

Equations (2) and (3) are used to generate interpolated adaptive histogram equalisation for histograms (x,y). If (x,y) is considered as a pixel in an image with intensity i, then m_{ru} defines the right upper mapping, m_{rl} - right lower mapping, m_{ru} - left upper mapping x^+, and m, the mapping of left lower x.

$$m(i) = a\left[b_m^-, i^- + (1-b)_m^+, i^-\right] + [1-a]\left[b_m^-, i^+ + (1-b)_m^+, i^+\right]$$

where $a = \frac{y - y^{-}}{y^{+} - y^{-}}$ and $b = \frac{x - x^{-}}{x^{+} - x^{-}}$

IV. RESULTS AND DISCUSSIONS

The datasets are collected from Kaggle repository from https://www.kaggle.com/datasets/vbookshelf/rice-leaf-diseases. The pre-processing is conducted in a python simulator with keras liberal that runs on a high-end computing system with 16 GB RAM with an i7 processor. The disease types used for finding out the efficacy of the pre-processing using Laplacian architecture is given below:

A. Bacterial leaf blight

Plants in rice fields become withered and their foliage turns yellow due to the presence of the bacterium Xanthomonas oryzae pv. oryzae. The principal origins of this sickness are the weeds and stubbles that have grown in the damaged area of the plant. Arid and irrigated areas are more vulnerable to its effects than other types of land. In the early stages of infection, the leaves are greyish green in colour and begin to fold inward. Symptoms of the disease include wilting and straw-colored leaves, which cause the seedlings to dry up and eventually die as the disease spreads.

0

Fig. 2. Bacterial leaf blight

B. Leaf brown spot

The fungus Cochliobolus miyabeanus is responsible for the development of Brown Spot. As a symptom, there are many big spots on the leaves that have the potential to devastate the entire leaf. If an infection arises in an immature seed, the result will be seeds that are unfilled, speckled, or discoloured. The lesions retain their circular shape as they expand in size, with a necrotic grey centre area and a reddish-brown to dark brown lesion edge that ranges from reddish-brown to dark brown.

Fig. 3. Leaf Brown Spot

C. Leaf blast

All rice fields are afflicted with the Magnaporthe oryzae fungus, which causes leaf blast and kills all of the rice plants. Blast disease is spread via infected areas, which are responsible for the disease emergence. As a result, soil moisture levels decrease, rain showers last longer, and temperatures drop. In the early stages, the lesions

or patches are white to gray-green in colour, with dark green borders around the perimeter. As the lesions progress, they take on the shape of an ellipse or a rod. Diamond-shaped lesions are characterised by white or grey centres that are bordered by reddish brown margins.

Fig. 4. Leaf Blast

D. Leaf streak

Leaf streak is caused by the bacterium Xanthomonas oryzae pv. oryzicola. There appears to be a lack of moisture in the leaves of the rice plants that have been harmed. Hot, humid areas are more likely to see bacterial leaf streaks. Linear lesions between leaf veins first show as dark green lesions, but as the disease progresses, the lesions turn light brown or yellowish grey in appearance.

Fig. 5. Leaf Streak

E. False smut

Because of the silkiness of the grain, a fake smut is created, which reduces the grain weight. Seed germination is also hindered as a result of this. The growth of the fake smut happens in areas where there is a lot of rain, high humidity, and a lot of nitrogen in the soil. The disease spores were also carried from one plant to another by the wind. This can only be seen after a panic episode has taken place, though. When it comes to the blossoming stage, it makes a difference.

Fig. 6. False Smut

The results of the proposed pre-processing method is tested in terms of image enhancement using various metrics that includes

- Measure of Enhancement (EME),
- Absolute Mean Brightness Error (AMBE),
- Measure of Enhancement by Entropy (EMEE),
- Tenengrad Measurement (TM) and
- Contrast Improvement Index (CII)

TABLE 1: PERFORMANCE ANALYSIS

Enhancement Techniques	AMBE	EME	EMEE	TM	CII
AHE-Median	$9.60e^{+01}$	$5.56e^{-01}$	$9.2e^{-04}$	$7.37e^{-04}$	$6.44e^{-03}$
AHE-Weiner	$2.35e^{+01}$	$4.42e^{-01}$	$9.3e^{-04}$	$2.27e^{-04}$	$4.80e^{-03}$
AHE- Non-Local Means	$4.63e^{+00}$	$1.40e^{-01}$	$9.86e^{-04}$	$3.28e^{-04}$	$3.58e^{-03}$
AHE-LP	$9.96e^{+00}$	$1.96e^{-01}$	$8.33e^{-04}$	$1.11e^{-04}$	$9.05e^{-04}$

Table 1 shows the results of various performance metrics that includes AMBE, EME, EMEE, CII and TM against AHE-Median, AHE-Weiner, AHE- Non-Local Means and AHE-LP. The results of simulation shows that the proposed method achieves better enhancement in terms of higher AMBE, reduced EME, higher EMEE, reduced TM and minimal CII. The results further shows that proposed method performs with enhanced image enhancement than other methods. The illustration of which are given in Fig. 7 – 11

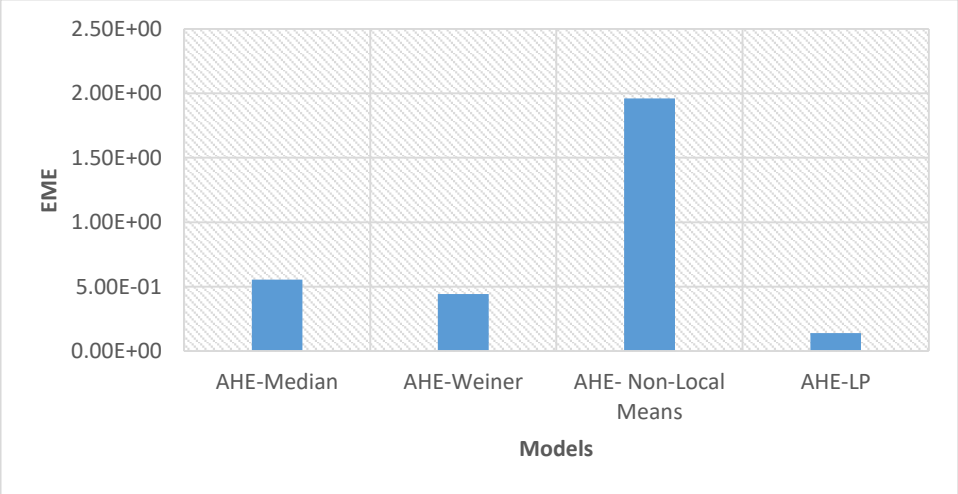

Fig. 7. Measure of Enhancement (EME)

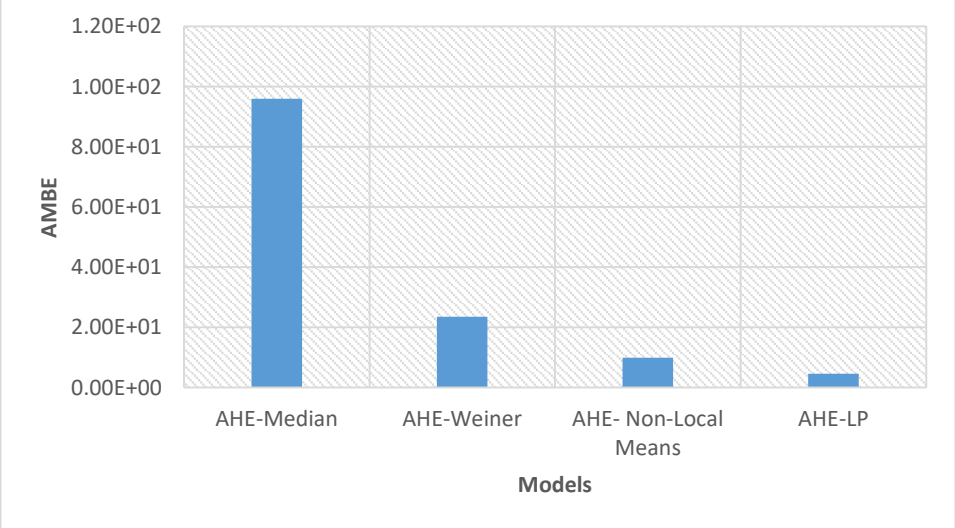

Fig. 8. Absolute Mean Brightness Error (AMBE)

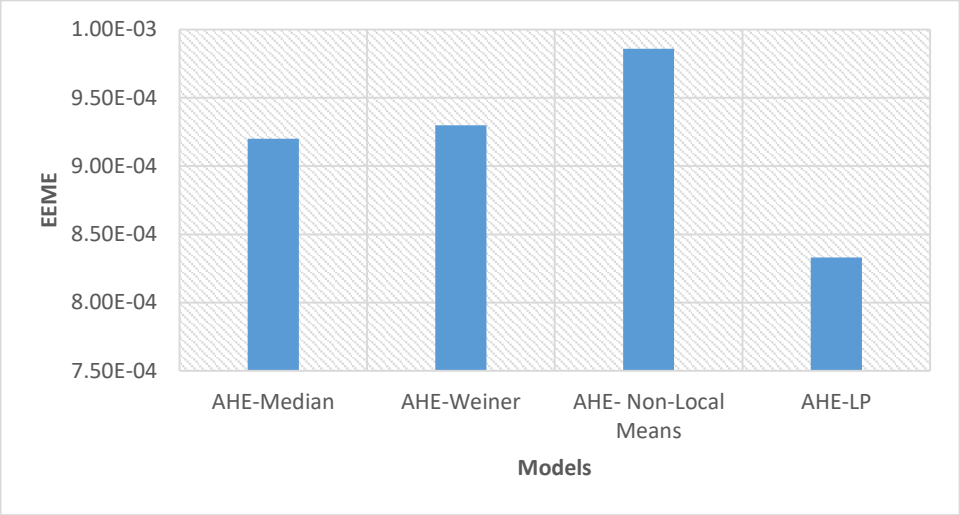

Fig. 9. Measure of Enhancement by Entropy (EMEE)

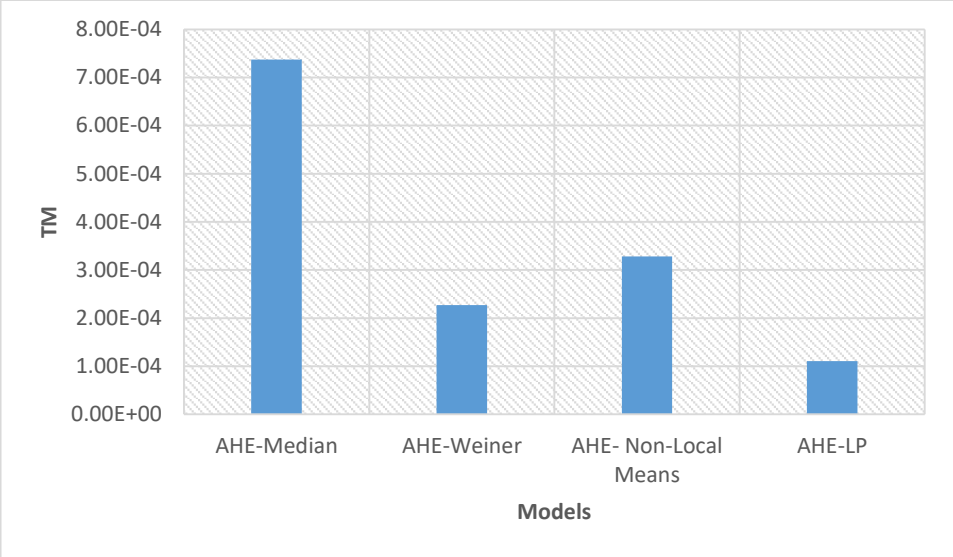

Fig. 10. Tenengrad Measurement (TM)

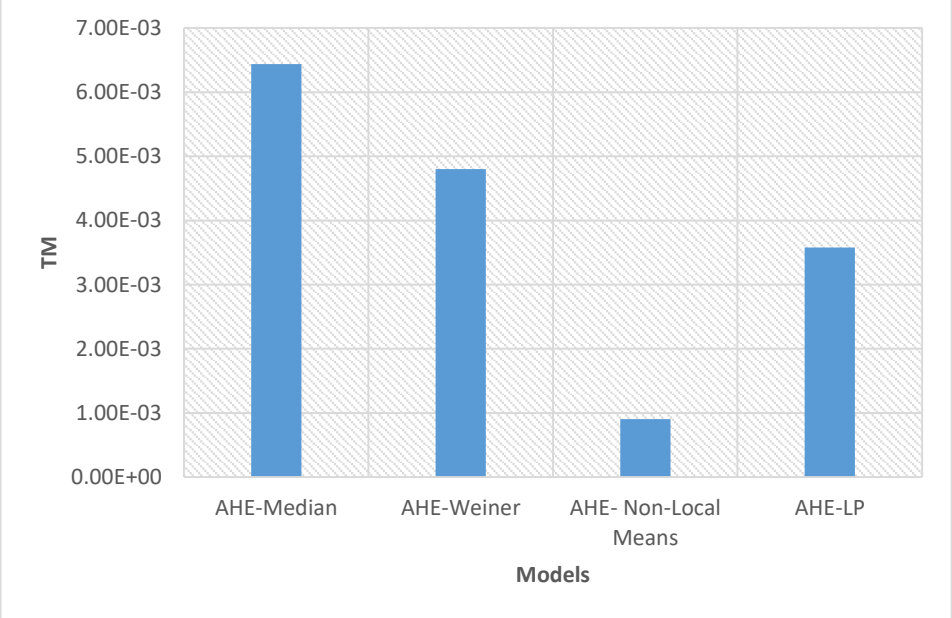

Fig. 11. Contrast Improvement Index (CII)

V. CONCLUSIONS AND FUTURE WORK

This study employs a Laplacian filter to reduce unwanted noise from images before extracting the features using a generalized linear convolutional model (GLCM). A computer simulation is used to evaluate the proposed methodologies for preprocessing and feature extraction, and the results are presented. According to simulation data, this technique looks to be superior to others in terms of boosting the accuracy of diagnosing the entire plant, as opposed to other strategies.

REFERENCES

1. Manohar, N., & Gowda, K. J. (2020, July). Image Processing System based Identification and Classification of Leaf Disease: A Case Study on Paddy Leaf. In 2020 International Conference on Electronics and Sustainable Communication Systems (ICESC) (pp. 451-457). IEEE.
2. Patil, N. S. (2021). Identification of Paddy Leaf Diseases using Evolutionary and Machine Learning Methods. Turkish Journal of Computer and Mathematics Education (TURCOMAT), 12(2), 1672-1686.
3. Julie, J., Athanesious, J. J., & Adharsh, S. (2021, December). Novel Disease detection for paddy crop using CNN with Transfer Learning. In 2021 4th International Conference on Computing and Communications Technologies (ICCCT) (pp. 252-255). IEEE.
4. Islam, R., & Islam, M. R. (2015). An image processing technique to calculate percentage of disease affected pixels of paddy leaf. International Journal of Computer Applications, 123(12).
5. Leelavathy, B., & Rao Kovvur, R. M. (2021). Prediction of biotic stress in paddy crop using deep convolutional neural networks. In Proceedings of International Conference on Computational Intelligence and Data Engineering (pp. 337-346). Springer, Singapore.
6. Wiling, B. (2017). Monitoring of Sona Massori Paddy Crop and its Pests Using Image Processing. International Journal of New Practices in Management and Engineering, 6(02), 01-06.
7. Radhakrishnan, S. (2020). An improved machine learning algorithm for predicting blast disease in paddy crop. Materials Today: Proceedings, 33, 682-686.
8. Malathi, V., & Gopinath, M. P. (2020). Noise Deduction in Novel Paddy Data Repository using Filtering Techniques. Scalable Computing: Practice and Experience, 21(4), 601-610.
9. Sharma, R., & Singh, A. (2021). Image Pre-Processing and Paddy Pests Detection Using Tensorflow. In Machine Learning and Data Analytics for Predicting, Managing, and Monitoring Disease (pp. 131-139). IGI Global.
10. Calderon, S., Fallas, F., Zumbado, M., Tyrrell, P. N., Stark, H., Emersic, Z., ... & Solis, M. (2018, October). Assessing the impact of the deceived non local means filter as a preprocessing stage in a convolutional neural network based approach for age estimation using digital hand x-ray images. In 2018 25th IEEE International Conference on Image Processing (ICIP) (pp. 1752-1756). IEEE.
11. Choi, H., & Jeong, J. (2018). Despeckling images using a preprocessing filter and discrete wavelet transform-based noise reduction techniques. IEEE Sensors Journal, 18(8), 3131-3139.
12. Khan, K. B., Khaliq, A. A., Jalil, A., & Shahid, M. (2018). A robust technique based on VLM and Frangi filter for retinal vessel extraction and denoising. PloS one, 13(2), e0192203.
13. Nair, R. R., David, E., & Rajagopal, S. (2019). A robust anisotropic diffusion filter with low arithmetic complexity for images. EURASIP Journal on Image and Video Processing, 2019(1), 1-14.
14. Shabeer, S., Jayaraju, M., & Sheeba, O. (2020, April). The investigation study on non-linear filter based preprocessing for MRI image segmentation and classification. In AIP Conference Proceedings (Vol. 2222, No. 1, p. 030014). AIP Publishing LLC.
15. Yang, W., Li, Y., Liu, W., Chen, J., Li, C., & Men, Z. (2020). Scalloping Suppression for ScanSAR Images Based on Modified Kalman Filter With Preprocessing. IEEE Transactions on Geoscience and Remote Sensing, 59(9), 7535-7546.
16. Bnouni, N., Amor, H. B., Rekik, I., Rhim, M. S., Solaiman, B., & Amara, N. E. B. (2021, March). Boosting CNN Learning by Ensemble Image Preprocessing Methods for Cervical Cancer Segmentation. In 2021 18th International Multi-Conference on Systems, Signals & Devices (SSD) (pp. 264-269). IEEE.